Ajou Med J 1999; 4(1): 9-14

# Chondroitin Sulfate Iron Colloid-enhanced MRI in Detection of Tumor Lesions in Patients with Hepatocellular Carcinoma: Comparison with Conventional MRI and CT during Arterial Portography (CTAP)

Young Soo Kim, Young Jun Shin, Kwang Jae Lee, Byung Mu Yoo
Sung Won Cho, Hoon Ji[1] and Yoon Mi Jin[2]

Departments of Gastroenterology, [1]Diagnostic Radiology and [2]Pathology
Ajou University School of Medicine, Suwon, Korea

Chondroitin sulfate iron colloid (CSIC)-enhanced MRI is a new method for the detection of hepatocellular carcinoma (HCC). After intravenous injection, CSIC is rapidly incorporated into Kupffer cells in the liver. The aim of this study is to investigate the value of CSIC-enhanced MRI in detection of HCC and to compare with conventional MRI and CTAP.

HCC was diagnosed by serum AFP, ultrasonograpy, conventional abdominal CT, and liver biopsy. Hepatic MR images were obtained before and one hour after finishing injection of CSIC in 22 patients with HCC. CT during arterial portography (CTAP) was obtained in 9 of 22 patients with HCC.

After injection of CSIC, signal intensity of normal hepatic tissue was decreased, whereas signal intensity of tumor was not changed as compared with conventional MRI, and tumor to liver contrast was increased in all patients. CSIC-enhanced MRI revealed a total of 82 HCC lesions, however conventional MRI revealed only 70 HCC lesions. Especially, when the lesion was less than 1 cm, CSIC-enhanced MRI showed ten additional lesions compared with conventional MRI. Comparing with conventional MRI and CSIC-enhanced MRI, CTAP showed four and two more lesions, respectively.

Our results suggested that CSIC-enhanced MRI was comparable to CTAP in the detection of HCC, and, compared with conventional MRI, it increased the detection rate of small HCC, especially those less than 1 cm in diameter. (Ajou Med J 1999; 4(1): 9~14)

**Key Words:** *Chondroitin sulfate iron colloid, MRI, Hepatocellular carcinoma*

## INTRODUCTION

Magnetic resonance imaging (MRI) is useful for the detection of hepatocellular carcinoma (HCC), and new contrast agents such as gadopentetate dimeglumine (Gd-DTPA), mangafodir trisodium (Mn-DPDP), and Fe-EHPG (iron ethylenebis-2-hydro-phenylglycine) have been developed to improve the delineation of HCC, but they are rarely sufficient contrasts for the detection of small tumors.[1,2] Iron colloidal superparamagnetic particles, such as ferrite particles, reduce the signal intensity of normal hepatic tissues by being taken up into hepatic reticuloendothelial cells, Kupffer cells. They are not taken into portion of tumors without Kupffer cells. Thus, contrast between tumor and normal liver tissue is enhanced.[3~6] CSIC is widely used intravenously in the treatment of anemia and its safety has been established in Japan.[7] Following intravenous injection, it is rapidly incorporated mainly into Kupffer cells in the liver.[5] CSIC is a stable iron colloid preparation with a trivalent iron ion. It is a paramagnetic substance with a molecular formula $[(C_{13}H_{19}O_{14}NS)\text{-}Fe(OH)_3]_n$, $n=150\sim160$, and the mean

**Reprint requests to:** Young Soo Kim, Department of Gastroenterology, Ajou University School of Medicine, San 5 Wonchon-Dong, Paldal-Gu, Suwon 442-749, Korea, Tel: 0331) 219-5720, Fax: 0331) 219-5999

molecular weight of 75 kDa. The particle size is 10 nm in dry state (by electron microscopy) and more than 100 nm in water (by ultrafiltration). The iron concentration of the preparation is 4 mg/ml (71.6 mM).[8]

After phagocytosis or processing by cells, it is metabolized as physiological iron.[9] CSIC is taken up in a short time by the liver with normal reticuloendothelial cells, and T2 relaxation time is shortened and signal intensity of the liver tissue is reduced in MRI. This is regarded as a T2-shortening effect.[10]

In liver tumors such as HCC, where reticuloendothelial function is impaired or absent, the signal intensity of the lesion relative to normal liver is increased after administration of CSIC. This may improve detection of liver tumors by enhancing tumor-to-liver contrast in MRI.[11] In the past, comparative study of CSIC-enhanced MRI with CTAP in detection of HCC was carried out in Japan, but they did not compare CSIC-enhanced MRI with conventional MRI simultaneously.

The aim of this study was to evaluate usefulness of CSIC-enhanced MRI in the detection of HCC and to compare with conventional MRI and computed tomography during arterial portography (CTAP).

## MATERIALS AND METHODS

The subjects were 22 patients with HCC, diagnosed by serum AFP, ultrasonography, conventional abdominal CT and liver biopsy. Of 22 patients, twelve patients were resected. Each subject gave written consent to participate in the study. MR images were performed with a Signa 1.5T system (General Electric Medical Systems, Milwaukee, Wisconsin, USA). Using the spin echo (SE) sequence, T1-weighted images (T1WI; TR/TE=500/9 ms), T2-weighted images (T2WI; TR/TE=2000/90 ms), proton density-weighted images (PDWI; TR/TE=2000/30 ms), and T2 fast spin echo images (T2FSE; TR/TE=4444/96 ms) were obtained. The slice thickness was 10 mm with a 2 mm gap. The field of view was 370 mm, and 192×256 for T1-weighted images, and 160×256 for T2-weighted images and proton density-weighted images. MR images were obtained before and one hour after finishing injection of CSIC (Blutal; Dianippon Pharmaceuticals, Osaka, Japan) under the same imaging condition. For each patient, 20 ml (80 mg $Fe^{2+}$) of CSIC was intravenously injected.[11] There were no side effects in all patients after injection of CSIC. Images of liver tumors were analyzed using an operator-defined region of interest (ROI). ROIs were set in the tumor region and in the liver parenchyma. The mean signal intensities (SI) per pixel were calculated for each region. The ROIs were 100 pixels in size. Background noise was measured as the standard deviation (SD) of SI in the corner of each image over a rectangular ROI including about 200 pixels. The signal-to-noise ratios (SNR) for the liver and tumor regions and the tumor to liver contrast-to-noise ratio (CNR) were calculated using the following formulae.[12]

$$\text{SNR liver} = \frac{\text{SI liver}}{\text{SD background}}$$

$$\text{SNR tumor} = \frac{\text{SI tumor}}{\text{SD background}}$$

$$\text{CNR} = \frac{\text{(SI tumor-SI liver)}}{\text{SD background}}$$

The paired *t*-test was used for statistical analysis of SNR and CNR before and after administration of CSIC, and $p<0.05$ were considered to indicate statistical significance. Dual phase abdominal CT scan was conducted with a high speed advantage system (General Electric Co. Milwaukee, Wisconsin, USA), with a 10 mm slice thickness, 10 mm table increments and an imaging time of 1.0 sec. After injection of 125 ml of contrast medium (Optiray, Mallinckrodt Medica, Inc., St. Louis, USA) at a rate of 2~3 ml/s, scanning of the entire liver was performed at 32 sec and 120 sec by the spiral volumetric CT technique. For CTAP, 60 ml of nonionic contrast material (Hexabrix, Andre Guerbet, Aulnay-Sous-Bois, France) was injected at a rate of 1.5 ml/sec via a catheter placed in the superior mesenteric artery. Imaging was initiated 25 to 30 sec after the start of injection, and 15 to 17 sequential images of the whole liver were obtained. We retrospectively reviewed conventional MRI, CSIC-enhanced MRI and CTAP simultaneously, and determined whether individual lesions could be detected by visual inspection. The sensitivities of imaging modalities were calculated on the basis of radiological findings. The specificities of imaging modalities were not estimated since false-positive and true-negative imaging findings could not be accurately correlated with

resected specimens in 12 of 22 patients.

## RESULTS

In MRI, the SNR in the liver after administration of CSIC was lower than before administration of CSIC on T2WI, PDWI and T2FSE (Table 1, Fig. 1). But no significant differences in SNR in tumor region were observed on all spin echo images(data not shown). The tumor to liver CNR obtained after administration was significantly higher than before administration of CSIC on T2WI, PDWI and T2FSE (Table 2, Fig. 2). This result on CSIC-enhanced MRI improved the detection rate of HCC. CSIC-enhanced MRI revealed a total of 82 HCC lesions, but, conventional MRI revealed only 70 HCC lesions. Especially, when the lesion was less than 1 cm, CSIC-enhanced MRI showed a total of 41 HCC lesions including 10 additional lesions compared with only 31 HCC lesions by conventional MRI (Table 3, Fig. 3). Detection rate of the lesion of less than 1 cm showed

**Table 1.** Signal to noise ratio (SNR) of surrounding liver parenchyma before and after administration of CSIC in 22 patients with hepatocellular carcinoma

| Images | Before | After |
|---|---|---|
| T1WI | 22.45±6.92[a] | 20.82±6.86 |
| T2WI | 8.45±3.65 | 5.47±2.41* |
| PDWI | 22.31±8.12 | 18.47±6.01* |
| T2FSE | 7.64±4.01 | 6.14±2.26* |

[a]mean±SD, *p<.05 compared with precontrast images.

**Table 2.** Tumor to liver contrast-noise ratio (CNR) before and after administration of CSIC in 22 patients with hepatocellular carcinoma

| Images | Before | After |
|---|---|---|
| T1WI | −7.88±2.94[a] | −6.02±6.86 |
| T2WI | 8.76±3.21 | 13.43±4.08* |
| PDWI | 6.21±2.76 | 16.02±5.32* |
| T2FSE | 19.01±6.16 | 23.07±6.83* |

[a]mean±SD, *p<.05 compared with precontrast images.

**Table 3.** Detection of tumor lesions in 22 patients with hepatocellular carcinoma by conventional MRI, CSIC-enhanced MRI and CTAP

| Imaging | No. of lesions | Detectable | | | |
|---|---|---|---|---|---|
| Diameter (cm) | | <1.0 | 1.0-<2.0 | 2.0-<3.0 | ≥3.0 |
| MRI | 70 | 31 | 13 | 12 | 14 |
| CSIC-MRI | 82 | 41* | 14 | 13 | 14 |
| MRI[a] | 30 | 18 | 6 | 3 | 3 |
| CSIC-MRI[a] | 32 | 20 | 6 | 3 | 3 |
| CTAP[a] | 34 | 20 | 8 | 3 | 3 |

[a]Nine of 22 patients with HCC were compared.
*p<.05 compared with conventional MRI by chi-square test.

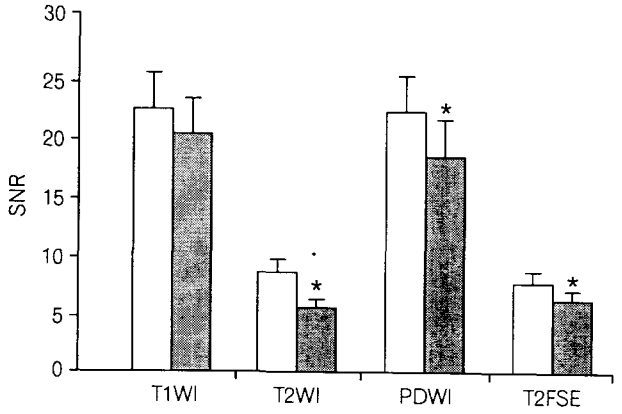


**Fig. 1.** Signal-to-noise ratio (SNR) of surrounding liver parenchyma in the 22 patients with hepatocellular carcinoma. When compared with SNR before administration of CSIC, there were significant decreases of SNR after administration. Data are expressed as mean±SD. *p<0.05.

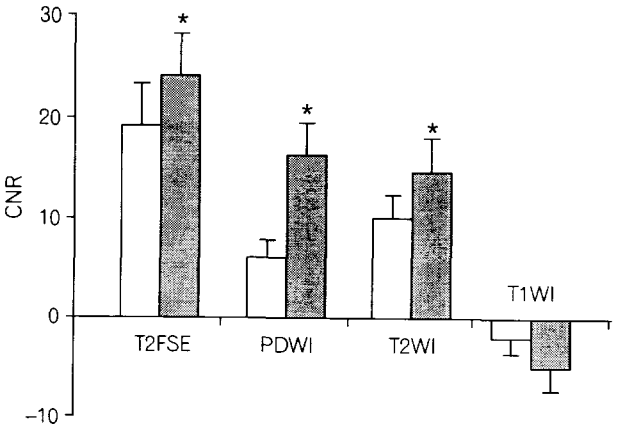


**Fig. 2.** Tumor to liver contrast-to-noise ratio (CNR) in the 22 patients with hepatocellular carcinoma. When compared with CNR before administration of CSIC, there were significant increases of CNR after administration. Data are expressed as mean±SD. *p<0.05.

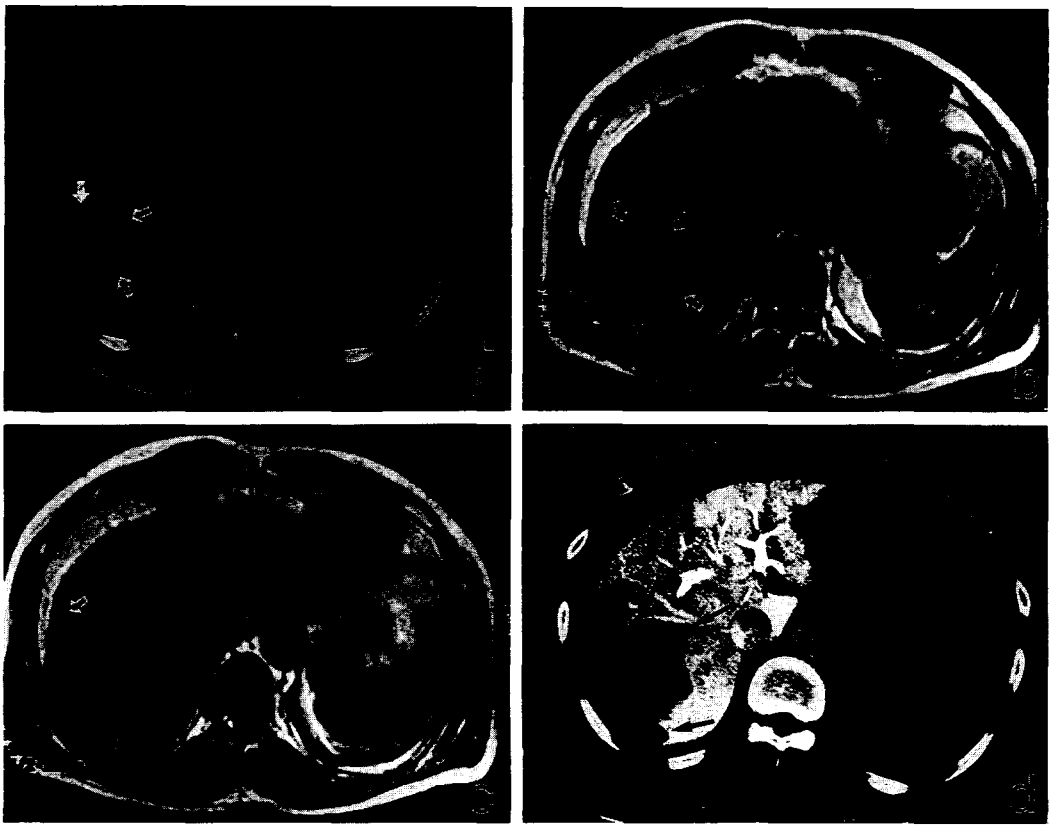

**Fig. 3.** (a) Conventional CT showed a large hypodense area without satellite lesions in the right lobe of liver (arrows). (b) Conventional proton density-weighted MR image revealed a hyperintense mass lesion (arrows). Another small hyperintense lesion was noted in the posterior area of the main mass (blank arrow). (c) CSIC-enhanced proton density-weighted MR image showed a hyperintense mass with small hyperintense lesion dorsal to the main mass (blank arrow). Another hyperintense lesion ventral to the main mass was visualized (arrow). (d) CTAP revealed a large portal perfusion defect which was larger than the size of the lesion on MR image (arrows). Another hypoattenuated lesion ventral to the main defect was noted (small arrow).

statistically significant difference in sensitivity between conventional MRI and CSIC-enhanced MRI ($p<0.05$ by chi-square test). CTAP was obtained in 9 of 22 patients with HCC. Comparing with conventional MRI and CSIC-enhanced MRI, CTAP showed four and two more lesions, respectively. But no significant statistical difference in sensitivity was observed (Table 3, Fig. 4).

## DISCUSSION

Recent advances in ultrasound and CT have made it possible to detect HCC less than 2.0 cm in diameter. However, the imaging characteristics of HCC are occasionally nonspecific, and its differentiation from noncancerous small nodular lesions of the liver, regenerative nodules and adenomatous hyperplastic nodules in cirrhotic liver with ultrasonography, CT, and angiography is difficult.[13] CTAP is the most reliable imaging modality for detecting HCC, since almost all HCCs show an absence or a decrease of intranodular portal blood supply.[14] However, this procedure is an invasive method. Especially in patients with marked portosystemic shunting and/or laminar flow of contrast material, it is difficult to assess intranodular portal blood supply.[15] Our results show that CSIC-enhanced MRI may be comparable to CTAP in the detection of HCC. But, CTAP revealed false positive lesion because a wedge-shaped portal flow defect might contain another lesion. The ability to produce multiplanar images coupled with the rapid development of paramagnetic contrast agents will confer MRI with an advantage over other noninvasive techniques. Recent reports have

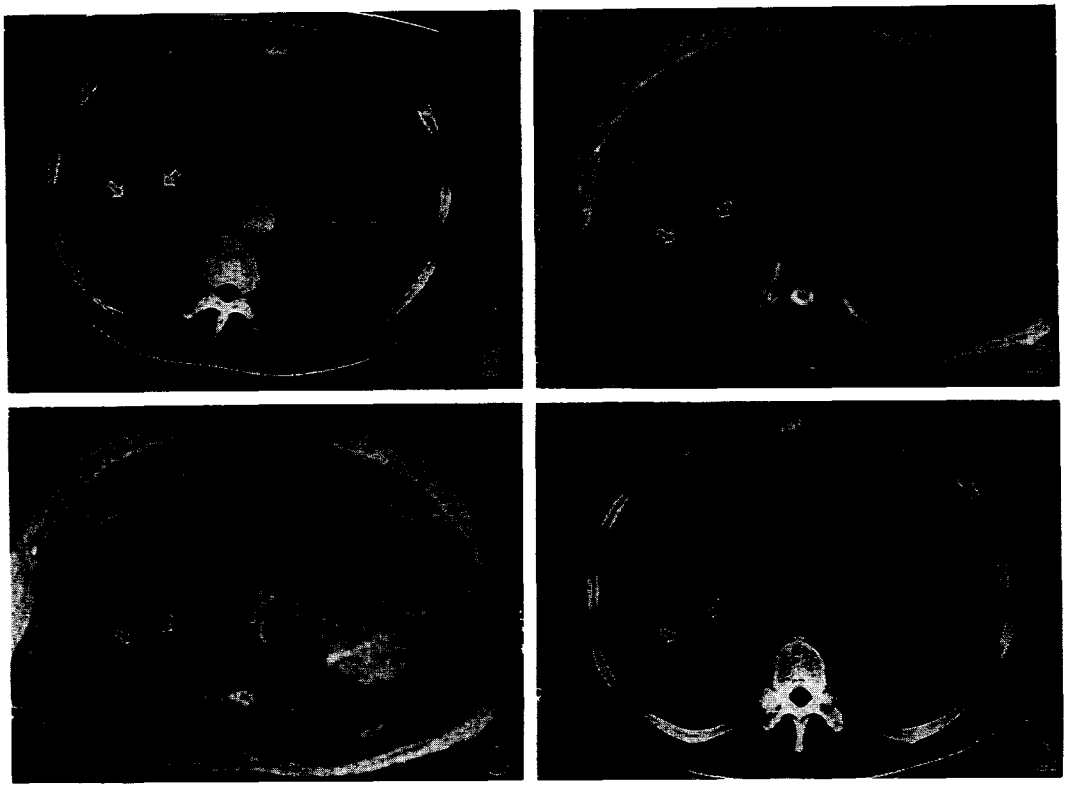

**Fig. 4.** (a) Conventional CT revealed a small hyperdense area in the right lobe of the liver (arrows). (b) Conventional T2-weighted image showed a subtle mass lesion in the right lobe of liver (arrows). (c) CSIC-enhanced T2-weighted image revealed a hyperintense mass lesion (arrows) with markedly decreased signal intensity of surrounding non-tumorous liver parenchyma. (d) CTAP revealed a small hypoattenuated portal perfusion defect in the right lobe of liver (arrows).

demonstrated that HCCs have a characteristic appearance on MRI. Characteristically, advanced HCC is usually hypo-intense on T1-weighted images and hyper-intense on T2-weighted images, similar to metastases. However, the signal intensity of HCC is more varied than that of other tumors, with hyper-intense or iso-intense T1-weighted images present in up to 30% of well-differentiated HCC.[16] Kato et al.[11] reported contrast-enhancing effect of CSIC in the male Wistar rats. Analysis of the iron concentration by atomic absorption spectrometry revealed that, while the iron concentration in the surrounding normal hepatic tissue was increased by CSIC injection, no significant increase in iron concentration in HCC was shown. As a consequence, a significant difference in iron level was noted between tumors and normal hepatic tissues. Studies on the possible use of CSIC as an MR contrast agent showed that CSIC could change the liver intensity at a dose range that could be administered to humans and was useful in the detection of small tumors in the liver.[17] CSIC uptake by the liver reached a maximum level between 15 minutes and 1 hour,[9,18,19] therefore, we performed CSIC-enhanced MRI 1 hour after CSIC injection. CSIC was incorporated into Kupffer cells in the liver, decreasing signal intensity of normal liver parenchyma. Since the number of Kupffer cells per unit volume were decreased in HCC, signal intensity was relatively increased and the tumor was depicted as a high intensity lesion.[17] Our data demonstrated CSIC-enhanced MRI was superior to conventional MRI in the detection of HCC lesions less than 1 cm, and CSIC was effective for improving the detectability of tumors. Previous report by Kamba et al.[15] showed that CSIC administration improved the detection by MR imaging of lesions less than 2 cm in diameter. CSIC-enhanced MRI may be useful in the screening of small HCC, especially less than 1 cm in diameter, because it is a less invasive procedure than CTAP, and it is superior to conventional MRI and comparable to CTAP in the detection of HCC. An another advantage of CSIC-

enhanced MRI is the ability to differentiate HCC from adenomatous hyperplasia. Suto et al.[17] reported CSIC-enhanced MRI is useful in differentiating adenomatous hyperplasia from HCC because Kupffer cells are abundant in adenomatous hyperplasia and the uptake of colloid is normal or increased. After intravenous injection of CSIC, the tumor-liver CNR decreased on T1-weighted images in adenomatous hyperplasia, and there was no significant change in CNR on T2-weighted images. In HCC, however, CNR increased on both T1- and T2-weighted images. CSIC-enhanced MRI also has an ability to predict the degree of differentiation of HCC on the basis of reticuloendothelial function of tumor cells. The number of reticuloendothelial cells in HCC differs according to the degree of differentiation.

The number has been reported to be lower in less differentiatied HCC. In moderately or poorly differentiated HCC, CNR is significantly increased after CSIC injection on both T1 weighted images and T2 weighted images.[20]

## CONCLUSIONS

CSIC-enhanced MRI was comparable to CTAP in the detection of HCC, and, compared with conventional MRI, it increased the detection rate of small HCC, especially those less than 1 cm in diameter.

## REFERENCES


1. Karani J: Imaging in liver disease. J Hepatol 25(1): 1-4, 1996
2. Suto Y and Shimatani Y: Dual contrast magnetic resonance imaging with combined use of positive and negative contrast agent in human hepatocellular carcinoma. Br J Radiol 68: 116-120, 1995
3. Saini S, Stark DD, Hahn PF, Bousquet JC, Introcasso J, Wittenberg J, Brady TJ and Ferrucci JT Jr.: Ferrite particles: a superparamagnetic MR contrast agent for enhanced detection of liver carcinoma. Radiology 162: 217-222, 1987
4. Tsang YM, Stark DD, Chen MCM, Weissleder R, Wittenberg J and Ferrucci JT: Hepatic micrometastases in the rat: ferrite-enhanced MR imaging. Radiology 167: 21-24, 1988
5. Kawamura Y, Endo K, Watanabe Y, Saga T, Nakai T, Hikita H, Kagawa K and Konishi J: Use of magnetite particles as a contrast agent for MR imaging of the liver. Radiology 174: 357-360, 1990
6. Weissleder R and Stark DD: Magnetic resonance imaging of liver tumors. Semin Ultrasound 10: 63-77, 1989
7. Nakanishi Y, Kurata K, Yoshimura Y and Oise S: Chondroitin sulfate iron colloid for intravenous injection (1st report). Physicochemical property and pharmacological significance. Yakugaku Zasshi 86: 46-50, 1966
8. Okuhata Y: An experimental study on MR lymphography with various iron colloid agents. Nippon Acta Radiol 52: 1148-1160, 1992
9. Nakanishi Y and Kishi M: Studies on iron-chondroitin sulfate colloid for intravenous injection. IV. Distribution of 59Fe in the mice followed by the injection of 59Fe labeled iron-chondroitin sulfate colloid. (2). Dose dependence of the distribution and the fractionation of 59Fe in organs. Yakugaku Zasshi 90: 120-126, 1970
10. Saini S, Frankel RB, Stark DD and Ferrucci JT Jr.: Magnetism: a primer and review. Am J Radiol 150: 735-743, 1988
11. Kato T, Suto Y and Matsuto T: Chondroitin sulfate iron colloid as an MR contrast agent for the hepatic reticuloendothelial system. J Comput Asst Tomogr 17: 603-608, 1993
12. Suto Y, Ametani M, Kamba M and Sugihara S: Time-course changes of contrast enhancement in iron colloid enhanced MRI in patients with hepatocellular carcinoma. Br J Radiol 69: 201-205, 1996
13. Matsui O, Kadoya M, Kameyama T, Yoshikawa J and Takashima T: Imaging diagnosis of hepatocellular carcinomas. Jpn J Cancer Chemother 16: 25-33, 1989
14. Matsui O, Kadoya M, Kameyama T, Yoshikawa J, Takashima T, Nakamura K, Unoura M, Kobayashi K, Izumi R and Ida M: Benign and malignant nodules in cirrhotic livers. Distinction based on blood supply. Radiology 178: 493-497, 1991
15. Kamba M, Suto Y and Kato T: Chondroitin sulfate iron colloid-enhanced MR imaging in patients with hepatocellular carcinoma; Comparison with CT during arterial portography. Acta Radiol 35: 570-575, 1994
16. Karani J: Imaging in liver disease. J Hepatol 25(1): 1-4, 1996
17. Suto Y, Kato T, Matsuo T, Kamba Y, Shimatani Y, Ohuchi Y, Nakamura K and Ohta Y: Chodroitin sulfate iron colloid as MR contrast agent in differentiation between hepatocellular carcinoma and adenomatous hyperplasia. Acta Radiol 34: 226-229, 1993
18. Kageyama J, Toyoma Y, Takashima H and Tanabe M: Possibility of chondroitin sulfate iron colloid sol as a contrast agent for magnetic resonance imaging. Igaku No Ayumi 158: 133-134, 1991
19. Nakanishi Y, Kishi M and Minagi Y: Studies on iron-chondroitin sulfate for intravenous injection. V. Distribution of $^{3}H$ in the mice followed by the injection of $^{3}H$ labeled iron-chondroitin sulfate colloid. Yakugaku Zasshi 90: 683-692, 1970
20. Suto Y, Kodama F, Kamba M and Ohta Y: Correlation between chondroitin sulphate iron colloid-enhanced MR imaging and the histological grade of hepatocellular carcinoma. Acta Radiol 36: 102-105, 1995